S.M. Raafat

Department of Control and System Engineering, University of Technology, Baghdad, Iraq.
60154@uotechnology.edu.iq

H.A. Ali

Collage of Al Hussain, Kerbala, Iraq.
zeugma20052000@yahoo.com

Received on: 10/05/2016
Accepted on: 23/02/2017

Robust Controller Analysis and Design of Medical Haptic Control System

Abstract-*Haptic interfaces for medial simulation prove to be especially useful for training in minimally invasive procedures. In this research, a framework that consists of relevant representation of operator and environment dynamic of a tele-manipulated haptic system is implemented. The uncertainty model of the operator and environment models is considered as well to study the influence on the aspects of stability and performance. The framework of H_∞ loop shaping robust controller design is applied, then the stability and performance analysis is investigated. Parametric robust control design method is used as well for comparison. The v-gap metric is considered to develop an accurate measurement of uncertainty. Based on the obtained value of the v-gap an efficient procedure of robust control design is applied. The obtained values of v- gap were 0.1112 for the master and $9.755*10^{-4}$ for the slave parts of the haptic system, which indicate improved robustness of stability and performance as compared with the obtained values from parametric robust controller design.*

Keywords-*haptic interface, tele-manipulator, H_∞ loop shaping, robust control, v-gap metric, master and slave.*

How to cite this article: S.M. Raafat and H.A. Ali, "Robust Controller Analysis and Design of Medical Haptic Control System," *Engineering and Technology Journal*, Vol. 35, Part A. No. 4, pp. 318-326, 2017.

1. Introduction

Advances of internet technology have greatly simplified remote acquisition and transfer of information for human. Assembling the internet and micromanipulation produces a new technology for humanoid that can sense and perform in a very far micro-environment. This novel technology has a prospective influence in many areas of applications that relates to the biological distant control treatment or the assemblage of Microsystems [1, 2]. Nevertheless, for effective and harmless systems, hypermedia information should be delivered to the operator. This hypermedia information will transfer human sense to a distant microenvironment via macro-micro bilateral tele-operation. The methodologies that take care of bilateral tele-operation with variable time delays are primarily centered on scattering principle formalism [3], the wave variable theory [4], or the sliding mode control [5]. These methodologies had complicated the handling of the uncertainty of the plant, measurement of noise, and disturbances applied to the system.

The performance of stability adjustment is the central decider of the control strategy for micro-tele-operation systems. On the other hand, robust control techniques proves to achieve guaranteed stability and performance against parameter variations and external disturbances [6-8]. Therefore, robust H_∞ control theory has been used to develop robust controllers and proved very useful for macro scale tele-operation [9], where H_∞ theory has been developed for bilateral controller without considering the effects of time delay. A robust framework for bilateral tele-manipulation had been suggested in [10], where the two-layer methodology permits the combination of passivity and transparency in an exactly spontaneous way. In [11], a time varying two-layer method with destabilizing factors had been applied in order to ensure stable performance of bilateral tele-manipulation systems. Wang and Xiao in 2013 proposed robust loop-shaping techniques for a two-axis nano-positioning piezoelectric phase, where it had been noticed that the nonlinear characteristics of piezoelectric materials could degrade the system performance [12]. In addition, the design and application of a robust Proportional Derivative (PD) controller has been proposed in 2014 [13], based on linear matrix inequality (LMI), in order to control a hub angular position and end-point deflection of a planar two-link flexible manipulator. The estimated PD gains had been applied to control the system in numerous loading situations.

In this paper, robust loop shaping H_∞ robust controller design is applied to a One Degree of Freedom (DOF) haptic system, as will be described in Section 2.The implemented robust

https://doi.org/10.30684/etj.35.4A.3
2412-0758/University of Technology-Iraq, Baghdad, Iraq

controller methodology is illustrated in Section 3, the effects of time delay are discussed in Section 4, Section 5 introduce the *v-gap* as combined with the robust loop shaping H_∞ controller design. Section 6 presents some simulation results, and some concluding comments are given in Section 7.

2. 1-DOF Haptic Force Feedback System, Mathematical Model

In this paper, a 1-DOF haptic device [14] is considered, as given in the following equations:

$$f = m(x)\ddot{x} + b(x)\dot{x} + k_c(x) + F_u \quad (1)$$

$$f - F_u = m(x)\ddot{x} + b(x)\dot{x} + k_c(x) \quad (2)$$

Where m is the mass matrix, b is the centrifugal and corelis forces and k_c is the gravitational force. F_u is the user contact force while x represents task space coordinates.

The applied torque to the motor (joint) can be obtained by Jacobian matrix, as [15].

$$fJ^T = \tau \quad (3)$$

Where J is Jacobian matrix and τ is the torque that applied to the motor

In order to feel the realistic contact forces and torque from the virtual environment, it is needed to include the user contact impedance in the impedance control structure of the haptic device.

The contact impedance model between the user and the haptic device can be obtained by spring model as given by

$$F_u = b\dot{x} + k\Delta x \quad (4)$$

Where, k and b represent the user stiffness coefficients and damping, respectively.$\dot{x}$ is the velocity of the Tool Center Point (*TCP*) while Δx is the change in position. Meanwhile, a force sensor is mounted to the TCP to measure the forces [9].

The standard tele-operator architecture consists of the macro-master control which is the haptic interface, the micro-slave control presented by the micro-manipulator, and the bilateral control presented by the channel of communication [1], as shown in Figure 1, where $(f_h and\, f_e)$ characterize the operator force signal and the external force from slave to master.$x_m \& x_s$ denot the location signal from the slave and master position, respectively.

It is required to analyze the performance of the above haptic control structures and to investigate stability issues. The main advantage of this structure is to simplify the robust controller design for both constrained motion and free motion [16], (as will be illustrated in details in Section 3).

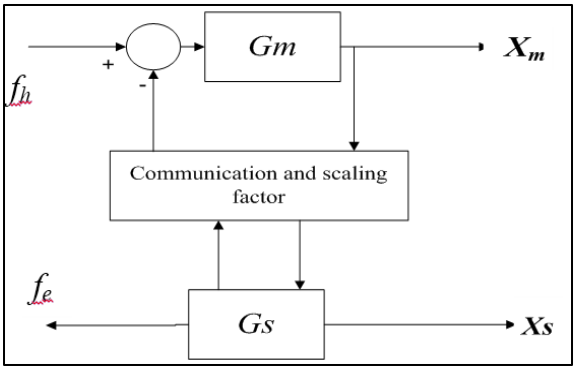

Figure 1: Block diagram of Haptic System [15]

3. Design of H_∞ Loop Shaping Robust Controller

The controller that can be applied for the tele-operation system is required to ensure stability robustness and fulfill optimal performance against multiple disturbances and uncertainties. Figure 2 refers to the structure of bilateral controller design based on loop-shaping. W_1, W_2 are weights and $G(s)$ is transfer function of system.

Based on normalized coprime factorization method of robust controller design [17], the problem of H_∞ robust stability is to find γ_{min} and *K(s)* stabilizing *G(s)* such that

$$\left\| \binom{I}{K} (1 - GK)^{-1} (I\ W2\ G\ W1) \right\|_\infty = \gamma_{min} = \varepsilon_{\max}^{-1} \quad (5)$$

Where the minimal value is given by

$$\gamma_{min} = \varepsilon_{max}^{-1} = \sqrt{1 + \lambda_{sup}(XY)} \quad (6)$$

The H_∞ robust loop shaping controller design for haptic system can be summarized as in the followings [18]:

I. The Method of Three-Stage Design

It is recommended to design a standard optimal controller (in one-step) that fills out all the requirements that seemed to be practically too conservative and leads to slight stability margins and placing constraints in the selection of the order of the weighting functions. The essential benefit is that both of the free motion and constrained motion can be worked out efficiently. The loop-shaping time delayed scaled tele-operator is shown in Figure 3. Where $P_m \& P_s$ are transfer function of master and slave, $K_m \& K_s$ are controller for master and slave $K, K_f \& K_P$ are bilateral control and scaling factors,$x_m \& x_e$ are

the position request from the master and the slave position, s_e is microenvironment, f_h & f_e are forces for operative and environment. The following steps specify procedure for controller design.

1. *Free Motion Controller Design:* The only considered case in the first stage is the case of free motion. In this case the master and the slave travel without restraint in the micromanipulation workplace where f_e=0. Any force exerted by the operator results in movement of the master and an equivalent movement of the slave. Eventually, the force/position transfer functions of master and slave can be defined at the formal effective point as [1].

$$P_m(s) = \frac{1}{m_m s^2 + k_m s + b_m} \quad (7)$$

$$P_s(s) = \frac{1}{m_s s^2 + k_s s + b_s} \quad (8)$$

Where m_m and m_s denote the mass of master and slave, $k_m$and $k_s$the compliance coefficients, $b_m$and b_s refer to the viscosity coefficients. The applied parameters are given in Table 1.
Figures 4 and 5 demonstrate the frequency responses of master system; the shaped master system "$W_{m1}.P_m.W_{m2}$" and the open-loop system "$W_{m1}.P_m.W_{m2}.K_m$". It's clear that the right margins of stability has been guaranteed by the shaping functions and K_m.

2. *Constrained Motion Controller Design:* The second stage concerns about the construction of a controller K for an "outer-loop" with forced motion, where the slave is in contact with the micro-environment and $f_e \neq 0$. A general scaled manipulator is recognized by a stationary motion scaling factor, "K_P," and a stationary-force scaling factor, "K_F", as shown in Equation 9 and Equation 10.

$$x_{m=} k_{\mathrm{p}}^{-1} x_s \quad (9)$$

$$f_{h=} k_f f_s \quad (10)$$

The master controller K_m is obtained by the command *ncfsyn* from "MATLAB"/ μ-analysis and synthesis toolbox [19]. In order to shape the plant with open loop the pre-filter and post-filter are consumed to attain a preferred frequency response in relation to certain definite design requirements like steady state error and bandwidth [19]. With the aim of confirming a low gain at high frequencies and a high gain at low frequencies, these weighting functions have been added: W_{m1}=(9s+5)/(0.02s+0.02), W_{m2}=1. This can be observed in the bode diagram of $W_{m1}.P_m.W_{m2}.K$, as shown in Figure 5, for free motion where f_e=0.

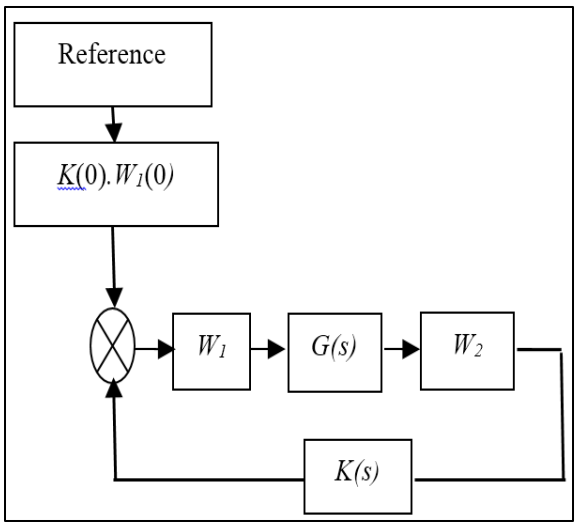

Figure 2: Loop-shaping design procedure [17]

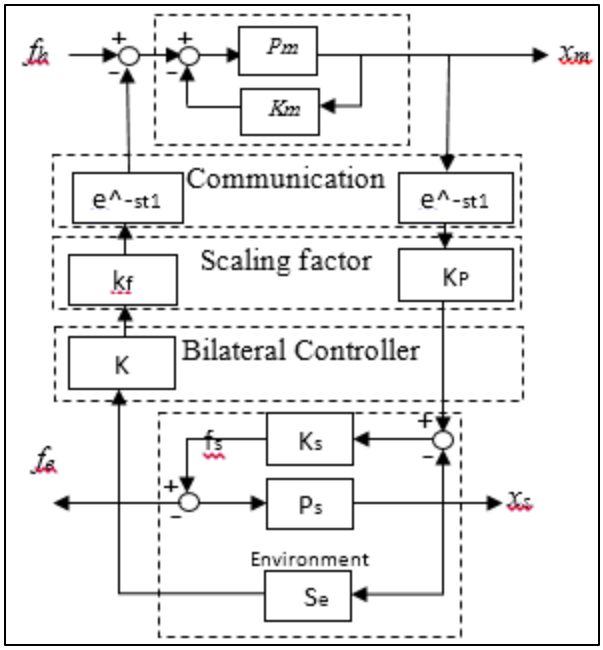

Figure 3: Bilateral Control including communication channel and scaling factors [17]

Table 1: master and slave parameter [17]

Master	m_m	k_m	b_m
	10.0	0.0	0.0
Slave	m_s	k_s	b_s
	4.88	$0.51 * 10^5$	$0.23 * 10^8$

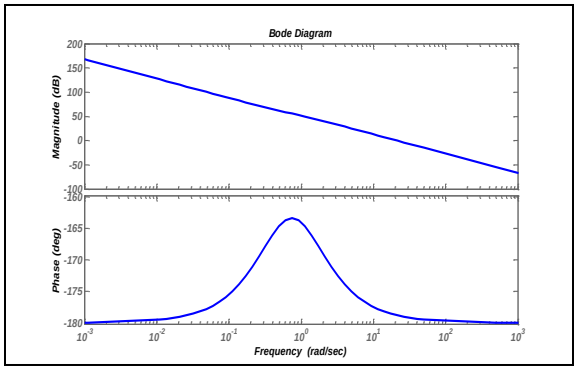

Figure 4: Bode diagram of $W_{m1}.P_m.W_{m2}$

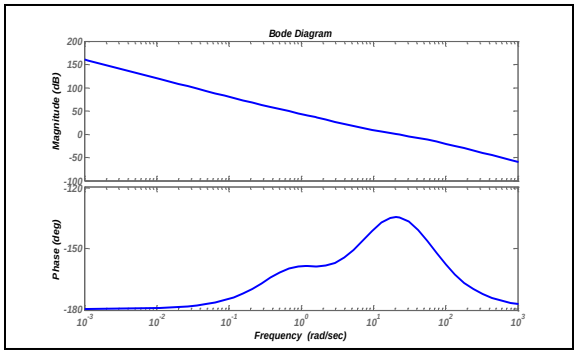

Figure 5: Bode diagram of $W_{m1}.P_m.W_{m2}.K_m$

II."H_∞ Loop-Shaping Control "Design for Micro-gripper

The system of slave consists of an *xyz*–platform micromanipulator and a two-fingered micro-gripper of piezoelectric material. The uncertain form of the device is formed with regard to its operating parameters; frequency, voltage and time. Robust stability and performance of the closed-loop controlled system in presence of model uncertainties should be attained. The model of the position of slave is tuned by the shaping functions W_{s1}, W_{s2}. Considering the behavior at low frequency of the micro-gripper, the shaping functions should be selected as W_{s1} and W_{s2} as given in Equation 11 and Equation 12 [17]:

$$W_{s1} = (585000s + 5)/(s) \quad (11)$$

$$W_{s2} = 1 \quad (12)$$

The slave controller K_s is gained for free movement, where f_e=0. Precise margins of stability can be guaranteed as shown in Figures 6 and 7 where the frequency responses of the shaped slave system $W_{s1}W_{s2}P_s$ and the "open-loop" system $W_{s1}W_{s2}P_sK_s$ are given. The resulted shape of the slave is slightly narrow at high frequencies where uncertainty due to unmodeled dynamics of actuator are present and wide at low frequencies where the presence of nonlinear hysteresis results in parametric uncertainty. On the other hand, the design and implementation of K_s does not have an impact on the performance of master system (i.e., K_m and P_m).

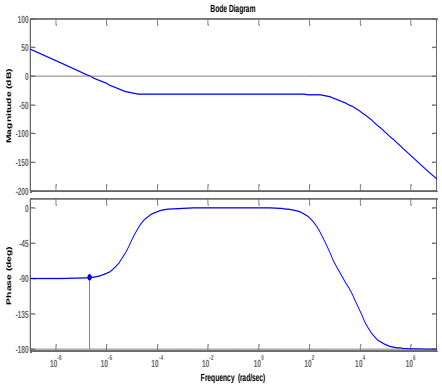

Figure 6: Bode diagram of $W_{s1}\ P_s\ W_{s2}$

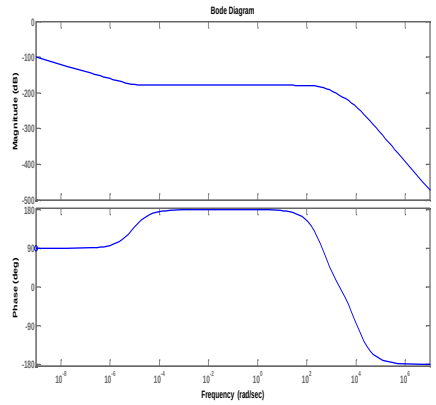

Figure7: Bode diagram of $W_{s1}\ P_s\ W_{s2}K_s$

III. H_∞-Loop-Shaping Bilateral Robust Controller

The bilateral controller design based on loop-shaping strategy can be illustrated as in Figure 8, and it can be described by the following closed-loop transfer function [17]

$$F_l(G,K) = \frac{K_P^{-1}W1G_mG_sW_TW_2}{1+K_P^{-1}W1K_fKG_mG_sW_TW_2} \quad (13)$$

$$G_m = \frac{APma}{PmaKm+1} \quad (14)$$

$$G_s = \frac{BKsPsaZe}{Psa(Ks+Ze)+1} \quad (15)$$

where $A = Km(0)W_{m2}(0)$, $PmaW_{m1}P_mW_{m2}$, $B = Ks(0)W_{s2}(0)$, $Psa = W_{s1}P_sW_{s2}$, $Z_e = \frac{K_e}{s} + b_es$ and $G = G_{m1}G_sW_T$.

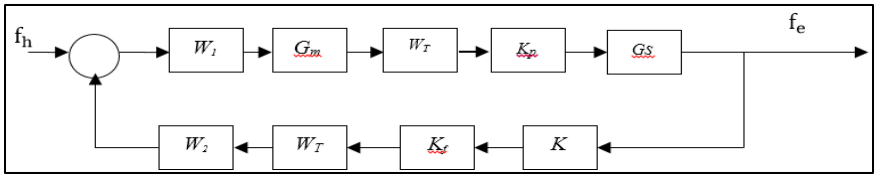

Figure 8: Bilateral controller *K* based on H_∞ loop shaping [17]

The frequency responses of the formed system $W_1.G.W_2$ and the dual controller including the right margins of stability of the tele-operation system are shown in Figure 9. When there is no contact force at the slave micro-gripper, the operation of the original system should not be affected by the inclusion of the bilateral controller. Eventually, the controller output is zero and has no effect on the processing of the motion system, f_e=0.

4. Effects of Time Delay

By integrating Equation (15) and Equation (14) into Equation (13), root locus analysis of the system will be possible. Figure 10 shows the root locus plot of time delay of 2 *sec*. It is clear that the system is stable for any value of scaling gain r_0 less than 2.1. Obviously, the value of r_0^c builds up as the time delay T_d decreases which permits the possibility of a broader, range as can be seen in Table 2.

A Padé approximation is needed to be used for the fixed communication time delay $W_t(s)=e^{-sT}$, where T is the time delay, so as to synthesize the robust dual controller. Differences in time delay are infinite-dimensional in polynomial space and cannot be revealed precisely in the model. In this paper, a Padé all-pass approximation [17] has been used as follows:

$$w_t(s)=e^{-sT}=\frac{e^{-sT/2}}{e^{+sT/2}}=\frac{1-\frac{sT}{2}-\frac{(sT)^2}{8}-\frac{(sT)^3}{48}}{1+\frac{sT}{2}+\frac{(sT)^2}{8}+\frac{(sT)^3}{48}} \qquad (16)$$

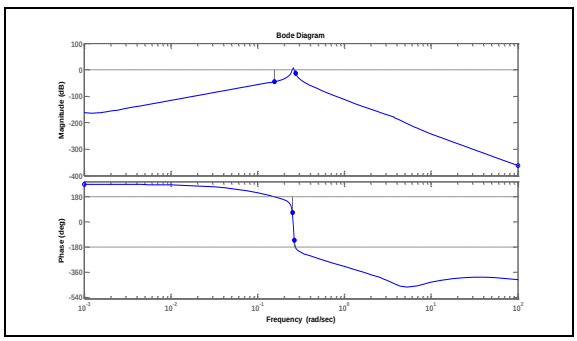

Figure 9: Bode diagram of W_1GW_2

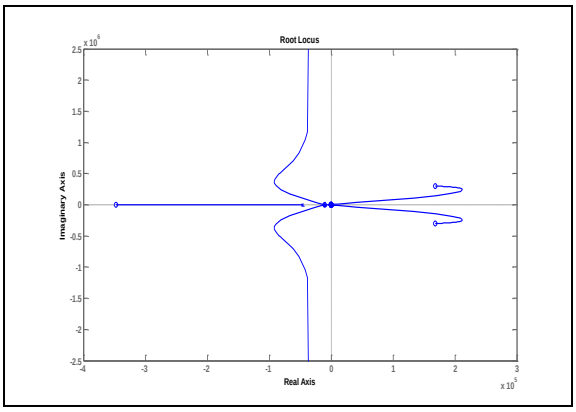

Figure 10: The time delay with root locus for *T*=2s

Table 2: Product of scaling r_0^c with upper bound

T(s)	2	1.75	1.5	1.25	1.0	0.5	0.25
r_0^c	2.1	2.37	2.81	3.3	4.22	7.77	11.1

5. H_∞ loop shaping and the ν-gap metric

The ν-gap metric is the maximum space between the frequency response loci of two systems; a nominal model of G_N and perturbed model G_i, respectively when plotted on the superficial of the Riemann sphere each time a specific winding number/encirclement is fulfilled [20]. According to the Proposition in [20] the ν- gap can be defined as:

$$\delta_v(G_N,G_i)\begin{cases} max_w M(G_N(e^{jw}),G_i(e^{jw})) & if \quad W(G_N,G_i)=0 \\ 1 & otherwise \end{cases} \qquad (17)$$

Where G_N is a nominal plant, G_i is the perturbed plant and $W(G_N,G_i)$ indicates the number of poles of G_k in the complement of the closed unit disc. Then, a controller K stabilizes G_N, also stabilizes G_i if this controller lies in the controller set:

$$\{K|b_{GN,K} > {}^{\delta}{}_{\nu}(G_N,G_i)\} \qquad (18)$$

Where $b_{GN,K}=min_w M(G_N(e^{jw}),\text{-}1/K(e^{jw}))$ is a general stability margin of the stable loop $[G_N,K]$. The scope of the set of controllers that ensures stability of both G_N and G_i is related to ${}^{\delta}{}_{\nu}(G_N,G_i)$. Consequently, the lesser the ν-gap between the nominal plant G_N and the disturbed

plant G_i, the bigger is the set of controller $G_N$that also stabilizes G_i. The gap values. The applied algorithm can be summarized as follows:
(**1**) Scaling inputs and outputs, so that a unit change on each input is significant in any case, similarly for outputs. (**2**) Plotting singular values of $G_N(j\omega)$ after scaling. (**3**) Inserting a pre-compensator $W(j\omega)$ consists of poles and zeros in Left Hand Poles (LHP)) to shape the singular values as required (e.g. proportional action diagonal pre-compensator). (**4**) Designing a controller K to maximize $b(G_NW,K)$ (say K_∞). If $b(G_NW,K_\infty)$ is≤0.2 then alter W and return to (3). (**5**) Implementing the controller WK_∞.
Table 3 shows the comparison between the H_∞ loop shaping robust controller based on *v*-gap and the robust controller based on parametric uncertainty between 20%-50%. It is obvious that the *v*-gap value obtained in the first method is more robust and accurate than the other method; e_{max} is much less with the master haptic system, b_{max} is higher in both the master and slave indicating a larger stability region, the gap metric is less and the order of the resulting control equation is lower which simplify the practical application.

6. Simulation Results

In order to test the proposed robust control performance, MATLAB program was prepared to accomplish simulated experiments. Figure 11 shows the step responses for the 1-DoF haptic master system. Figure 11-a demonstrates the instability of the system without controller while Figure 11-b shows the improved performance when the robust controller is added.
Figure 12-a represent the step response for the 1-DoF for haptic system for slave (without controller). Figure 12-b represents the step response for the 1-DoF for haptic system for slave with H_∞ contoller.
Then, another type of signal is used to test the robust control performance. Figure 13 represents sinusodal response the 1-DoF for haptic system for master (without controller K_m),while Figure 14 representes sinsodal response for master system with the robust controller. Figure 15 represented error response for master system with controller.

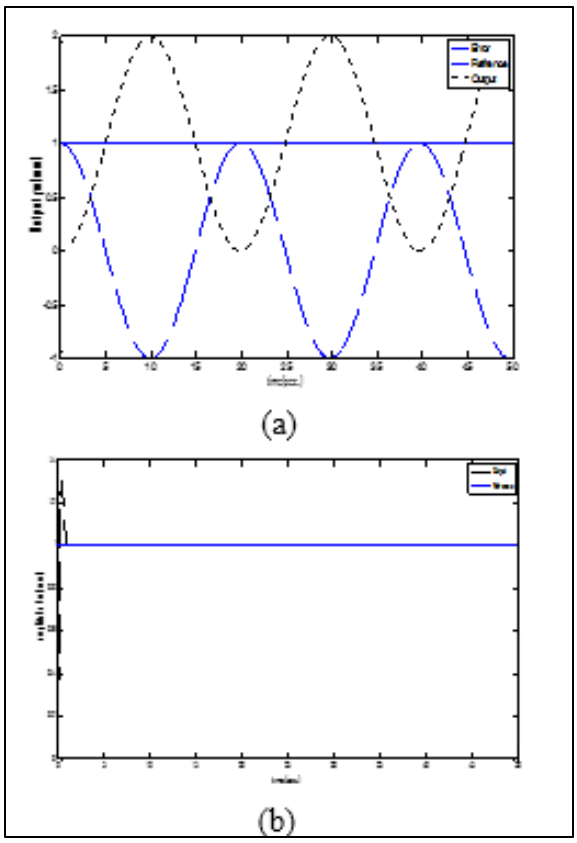

Figure 11: Step Response of the master part of the haptic system. *a*-without control, *b*-with robust control action

Table 3: comparison between the H_∞ loop shaping robust controller using *v*-gap and the robust controller based on parametric uncertainty

Haptic System	H_∞ loop shaping with *v*-gap metric	Controlled Haptic System With parametric uncertainty
Master-e_{max}	0.3827	0.7047
Master-γ=b_{max}	2.613	2.5814
Master-Transfer function of K	$\frac{2.414s - 3.162}{s + 7.634}$	$\frac{0.5914s^3 + 1.8252s^2 + 1.4797s + 0.360129}{0.0010s^4 + 1.5339s^3 + 5.4448 * s^2 + 5.6123s + 1.70036}$
Master-*v-gap* metric	0.1112	0.45
Slave-e_{max}	1	0.71596
Slave-γ =b_{max}	1	0.54
Slave-Transfer function of K	$\frac{-2.24410^{-6}s - 0.02271}{s + 1.09910^4}$	$\frac{0.0002s^2 + 1.8519s - 0.3455}{0.0106s^2 + 4.7582s}$
Slave-*v-gap*	9.7559e-004	0.8390

metric

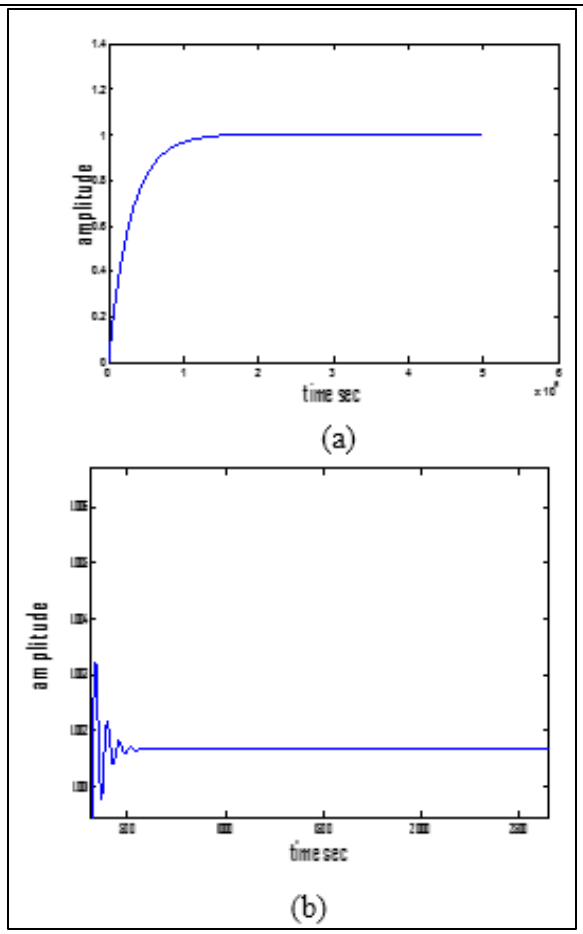

Figure 12: Step Response of the slave part of the haptic system. a-without control, b-with robust control action

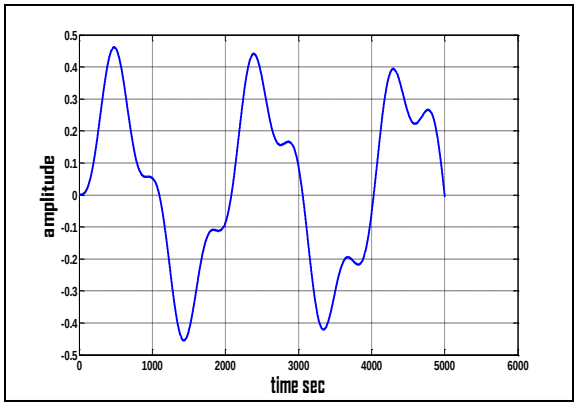

Figure13: Sinusoidal response for master without robust controller

Figure 16 shows the sinusoidal response for the 1-DoF for haptic system for slave (without controller K_s). Figure 17 depicts the sinusodal response for the 1-DoF for haptic system for slave (with controller K_s), and Figure 18 shows the error response for slave system.

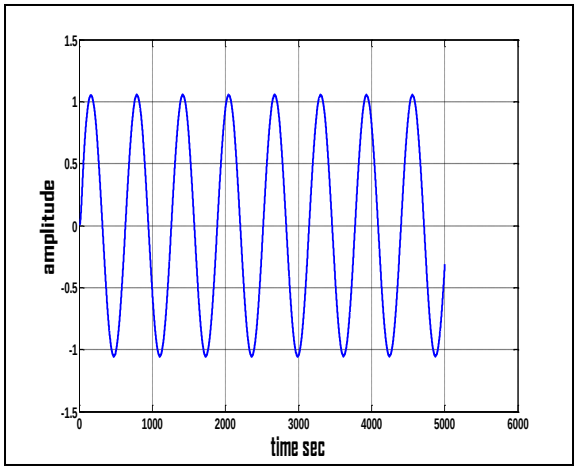

Figure 14: Sinusoidal response for master with robust controller

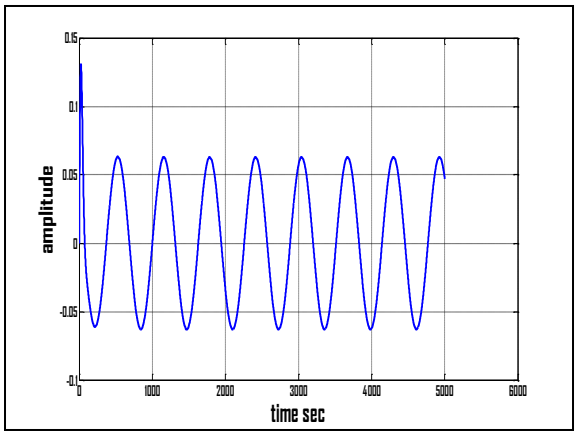

Figure 15: the error response for master system with robust controller

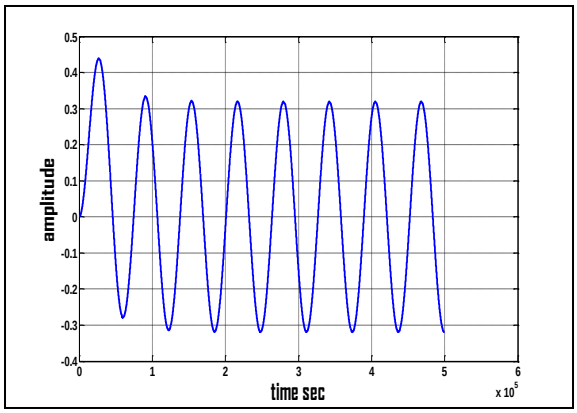

Figure 16: Sinusoidal response for slave without robust controller

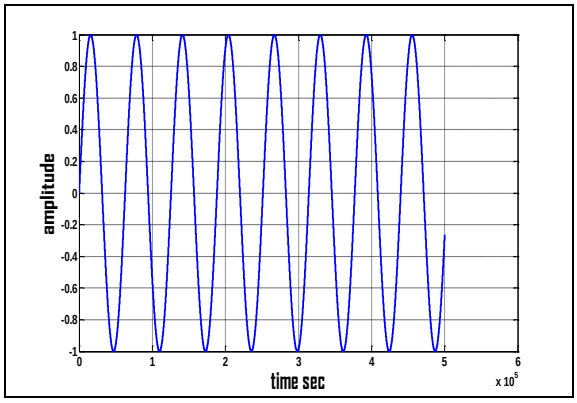

Figure 17: Sinusoidal response for slave with robust controller

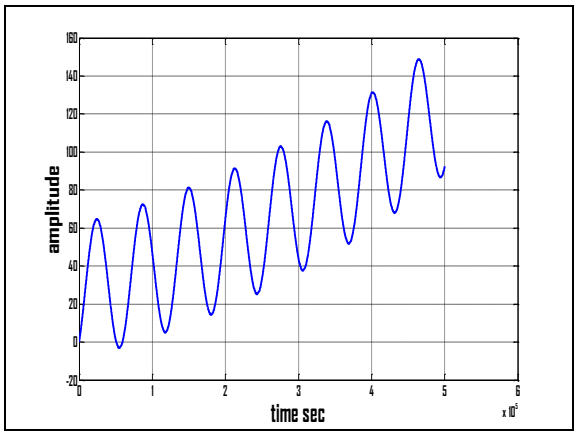

Figure 18: The error response for slave system with robust controller

7. Conclusion

In this work, the H_∞ loop shaping robust control with *v*-gap is applied for design and analysis of robust control for a 1-DOF of haptic system that can be used for medical applications. Simulation results show that when using the former controller the necessary conditions for robustness are satisfied under wide range of uncertainties and communication time delays. Robust stability against different time delays (up to two seconds) can been ensured by the application of the H_∞ loop shaping with *v-gap* procedure. Although the parametric uncertainty approach designed for a relatively large range of uncertainty (between 20%-50%) H_∞ loop shaping robust control with *v*-gap provides larger stability margin and precise system performance.

References

[1] N. Ando, P. Korondi, and H. Hashimoto, "Development of Micromanipulator and Haptic Interface for Networked Micromanipulation," *IEEE Trans. Mechatronics*, Vol. 6, No. 4, pp. 417–427, Dec. 2004.

[2] W.J. Li, "Internet-Based Remote Assembly of Micro-Electro-Mechanical Systems," *Assembly Autom.*, Vol. 24, No. 3, pp. 289–296, 2004.

[3] R.J. Anderson and M.W. Spong, "Bilateral Control of Teleoperators with Time Delay," *IEEE Trans. Autom. Control*, Vol. 34, No. 5, pp. 494–501, May 1989.

[4] G. Niemeyer and J.-J. E. Slotine, "Towards Force-Reflecting Tele-operation Over the Internet," in *Proc. IEEE Int. Conf. Robot. Autom.*, pp. 1909–1915, 1998.

[5] J.H. Park and H.C. Cho, "Sliding-Mode Controller for Bilateral Tele-operation with Varying Time Delay," in *Proc. IEEE/ASME Int. Conf. Adv. Intell. Mechatron*, pp. 311–316, 1999.

[6] H.I. Ali and A.H. Saeed, "Robust PI-PD Controller Design for Systems with Parametric Uncertainties", *Engineering and Technology Journal*, Vol. 34, Part A, No. 11, pp. 2167-2173, 2016.

[7] S.M. Raafat and R. Akmeliawati, "Intelligent H_2/H_∞ Robust Control of an Active Magnetic Bearings System," *Al-Khwarizmi Engineering Journal*, Vol. 11, No. 2, pp. 1- 12, pp. 1-11, 2015.

[8] H.I. Ali, "Robust PI-PD Controller Design for Magnetic Levitation System," *Engineering and Technology Journal*, Vol. 32, Part A, No.3, pp. 667-680, 2014.

[9] Z. Hu, S.E. Salcudean, "Robust Controller Design For Tele-operation Systems," in *Proc. IEEE Int. Conf. Syst., Man, Cybern.*, pp. 2127–2132,1995.

[10] M. Franken, "Friction Compensation in Energy-Based Bilateral Tele-manipulation," in Proc. *IEEE*/RSJ Int. Conf. Intell. Robots Syst., pp. 5264–5269, 2010.

[11] A.F. Rovers, "Design of A Robust Master-Slave Controller for Surgery Applications with Haptic Feedback," Eindhoven University of Technology, June 2003.

[12] A.R. Husain, "Vibration and Control," *IEEE Trans*. On Haptic, Vol 6, No 2, April -June 2013.

[13] Z. Mohamed, and B Subudhi Journal of "Vibration and Control", published online 18 June 2014.

[14] I. M. Buullock, "A Hand-Centric Classification of Human and Robot Dexterous Mainpulation," *IEEE Trans*. On Haptic, Vol. 6, No. 2, April -June 2013.

[15] D. Wang, and J. Xiao, "Configuration-Based Optimization for Six Degree of Freedom Hptic Rendering for Fine Manipulation," *IEEE Trans*. On Haptic, Vol. 6, No.2, April-June 2013.

[16] J. Scholtes, "Analysis of a Haptic Control Architecture, "University of Technology Eindhoven, June, 2009.

[17] M. Boukhnifer, A. Ferreira " H_∞ loop shaping Bilateral Controller for a Two-Fingered Tele-Micromanipulation Systems." *IEEE Trans. ON Control Systems Technology* , VOL. 15, NO. 5, September 2007.

[18] K. Glover and D. McFarlane, "Robust stabilization of normalized coprime factors: An explicit H_∞ solution," in *Proc. IEEE Amer. Control Conf.*, pp. 824–835, 1988.

[19] J. Doyle, K. Glover, P. Khargonekar, and B. Francis, "State-Space Solutions To Standard *H*and H_∞Control problems," *IEEE Trans. Autom.Control*, Vol. 34, No. 8, pp. 831–847, Aug. 1989.

[20] G. Vinnicombe. "Fixed Structure H_∞Control Design for Multiple Plants-A Coprime Factorization /LMI Based Approach," In Proceeding of European Control Conference Brussel, 1997.

Author(s) biography

Safanah M. Raafat, received her the B.Eng. and M.Sc. degrees in Control and System Engineering from the University of Technology-Baghdad, and Ph.D from Mechatronics Engineering at the International Islamic University Malaysia. Safanah has many publications on robust control and identification of uncertainties, sliding mode control, Extremum seeking control and real time scheduling. She is currently an assistant Professor of the Department of Control and System Engineering at University of Technology-Baghdad. Now she is a Senior Member of IEEE and a member of IEEE Control Systems Society. Her main research interests include System identification, optimization and optimal control, robust control systems theory and applications, intelligent system, robotics and positioning systems.

Hussein A. Ali received his the B.Eng. and M.Sc. Degrees in Control and System Engineering from the University of Technology–Baghdad, and work at Al-Husain University College.